α-NEM and model reduction

Francisco Chinesta, Elías Cueto, David Ryckelynck, Amine Ammar

▶ **To cite this version:**

Francisco Chinesta, Elías Cueto, David Ryckelynck, Amine Ammar. α-NEM and model reduction: Two new and powerful numerical techniques to describe flows involving short fibers suspensions. Revue Européenne des Éléments Finis, 2005, 14 (6-7), pp.903-923. 10.3166/reef.14.903-923 . hal-00020781

HAL Id: hal-00020781
https://hal.science/hal-00020781

Submitted on 26 Feb 2018

HAL is a multi-disciplinary open access archive for the deposit and dissemination of scientific research documents, whether they are published or not. The documents may come from teaching and research institutions in France or abroad, or from public or private research centers.

L'archive ouverte pluridisciplinaire **HAL**, est destinée au dépôt et à la diffusion de documents scientifiques de niveau recherche, publiés ou non, émanant des établissements d'enseignement et de recherche français ou étrangers, des laboratoires publics ou privés.

Distributed under a Creative Commons Attribution - NonCommercial 4.0 International License

α-NEM and model reduction: two new and powerful numerical techniques to describe flows involving short fibers suspensions

F. Chinesta[1], E. Cueto[2], D. Ryckelynck[1] and A. Ammar[3]

[1] *LMSP UMR 8106 CNRS-ENSAM-ESEM*
151 Boulevard de l'Hôpital, F-75013 Paris, France
francisco.chinesta@paris.ensam.fr
david.ryckelynck@paris.ensam.fr

[2] *Group of Structural Mechanics and Material Modelling. Institute of Engineering Research of Aragon (I3A).*
University of Zaragoza. Maria de Luna, 3. E-50018 Zaragoza, Spain.
ecueto@posta.unizar.es

[3] *Laboratoire de Rhéologie*
1301 rue de la piscine, BP 53 Domaine universitaire
38041 Grenoble Cedex 9, France
Amine.Ammar@ujf-grenoble.fr

ABSTRACT. *Numerical modeling of non-Newtonian flows typically involves the coupling between the equations of motion characterized by an elliptic character, and the fluid constitutive equation, which is an advection equation linked to the fluid history. In this work we propose a coupling between the natural element method which provides the capabilities of Lagrangian models to describe the flow front tracking as well as to treat the convection terms related to the fluid microstructure evolution - without the mesh quality requirements characteristics of the standard finite elements method - with a new approximation of the Fokker-Planck equation. This approximation is efficient and accurate, and is based on the use of an adaptive model reduction which couples the proper orthogonal decomposition (Karhunen-Loève) with an approximation basis enrichment based on the use of the Krylov subspaces, for describing the microstructure evolution.*

KEYWORDS: *Meshless techniques, Fokker-Planck equation, Molten composites, Model reduction*

1. Introduction

As a consequence of the increasing use of composite materials, there has been much work on constitutive equations and computational mechanics for short fibers composites. Since these materials are generally made of a matrix and fibers reinforcement, the mechanical properties of the conformed pieces depend greatly on the fibers orientation in the solid material. However, it turns out, that this orientation is determined by the forming process, so that it is interesting to develop mathematical models describing the flow during this conforming process and to develop specific numerical strategies to solve the resulting equations.

Mechanical modeling of short fibers suspensions flows is usually achieved in the framework of dilute or semi-dilute suspensions of non-spherical particles in a Newtonian fluid. The resulting system of equations involves the coupling of an elliptic problem with an advection problem related to the fluid history. The elliptic problem is associated with the equations of motion whereas the advection equation describes the time evolution of the anisotropic viscosity tensor (fiber orientation) or more generally the microstructural state. The second problem presents two difficulties: it is non-linear and hyperbolic (see the review paper from Azaiez et al., 2002).

Coupled models take into account both the dependence of the kinematics with the fiber orientation and the orientation induced by the flow kinematics. Usually the coupled models are solved by means of a fixed point strategy. In this case, at each iteration the flow kinematics results from the solution of motion and mass conservation equations, using the fiber orientation field from the previous iteration. From the kinematics just computed, the fiber orientation is updated solving the advection equation governing its evolution. Advection equations have been integrated by using any accurate numerical technique for hyperbolic equations: the method of characteristics, SUPG or discontinuous finite element techniques, discontinuous finite volumes, ... (Pironneau, 1989). Coupled models solving simultaneously the flow kinematics and the fiber orientation (fully coupled models) are rare in literature. The main difficulty in using fully coupled models is the distinct character of the model equations, which requires specific numerical techniques.

1.1. *The flow kinematics resolution*

The simulation of flows involving moving or free boundaries introduces specific difficulties related to the flow front treatment. A first possibility to describe the fluid volume evolution is the use of a fixed mesh strategy. In that case, the fluid volume updating is carried out from a control volume technique or by using a volume-of-fluid (VOF) technique, which introduces a new variable (the fluid presence function) whose evolution is governed, as described later, by a linear advection equation. Some of these techniques solve the flow kinematics exclusively in the fluid domain, whereas other ones operate in the whole domain imposing a pseudo-

behavior in the empty region (Azaiez et al., 2002). The use of this kind of techniques (fixed mesh strategies) induces additional difficulties in the flow front treatment, due to the fact that usual fixed mesh discretisation techniques update the fluid properties from their values at the previous time step. Thus, when an element starts its filling process, the variables related to the fluid, such as the temperature, the fiber orientation, ... are not defined in the empty elements, even though initial values are required to start the evolution process. Moreover, in all cases, the position and shape of the flow front is more or less uncertain, because in practice, during the filling simulation a great number of partially-filled elements appear. To improve the flow front location, some alternatives exist, as for example the level set method (Sussman et al., 1994), but its use is far to be trivial.

The consideration of a moving mesh strategy (as used for example in the Lagrangian finite element formulations) allows to get a good evaluation of the fluid domain evolution, although some precautions must be taken into account in the flow front tracking: confluent flow fronts, interaction of the flow front with the domain boundary, ... The advection equations related to the fluid history can be accurately integrated using the method of characteristics along the nodal trajectories. However, as it is well known in the context of the Lagrangian finite element method, the mesh becomes too distorted in few iterations to guarantee an accurate field interpolation in the mesh elements. In order to alleviate the remeshing constraint, some meshless methods have been proposed. However, usual meshless techniques do not define a nodal interpolation, and in consequence important difficulties are found in the application of the essential boundary conditions. The Natural Element Method – NEM- (Sukumar et al., 1998), is a novel meshless method, which has the property of nodal interpolation, and its accuracy does not depend on the regularity of nodal distribution, i.e. there is not geometrical restriction in the relative position of the nodes. Thus, if the NEM is used in the discretisation of the variational formulation of motion and mass conservation equations, the nodal position can be updated from the velocity field of the fluid, at the same time that advection equations are integrated using the method of characteristics. Even in the case of very irregular nodal distributions, when the solution can be interpolated by using the approximation functional basis, no remeshing is required. Nevertheless, the introduction or the elimination of some nodes is an easy task (Martinez et al., 2004).

1.2. *Description of the microstructure evolution*

As previously argued, "complex fluid" is the term commonly used to describe a wide class of liquid-like materials, in which the relaxation time towards the equilibrium state occurs sufficiently slowly that significant changes in the microstructural configuration, and thus in the macroscopic properties, can be induced by the flow. Viscoelastic fluids or short fiber suspensions may be considered as examples of complex fluids. The Fokker-Planck formalism is a commonly used -description of kinetic theory problems, for describing the evolution of the configuration distribution function. This function represents the probability of finding the microstructure element in a particular configuration.

In the case of a short fiber suspension, the configuration distribution function (also known as orientation distribution function) gives the probability of finding the fiber in a given direction. Obviously, this function depends on the physical coordinates (space and time) as well as on the configuration coordinates, that taking into account the rigid character of the fibers, are defined on the surface of the unit sphere. The evolution of the distribution function is given by the Fokker-Planck equation, that we introduce later.

We have proved in a former paper (Chiba et al., 2004) that in the context of the short fiber suspensions, the consideration of closure relations for deriving equations governing the evolution of different orientation tensors, can induce large deviations in the numerical solution with respect to the exact one. Thus, for example, in figure 1 we compare the solutions obtained solving the equation governing the evolution of the second order orientation tensor (which involves a quadratic closure relation) with the one obtained imposing the periodicity of the solution of the Fokker-Planck equation along the closed streamlines. The first solution has been computed using a stabilized Taylor Discontinuous Galerkin technique, whereas the second one makes use of a particle strategy. In these representations the fiber orientation distribution is illustrated with an ellipsoid.

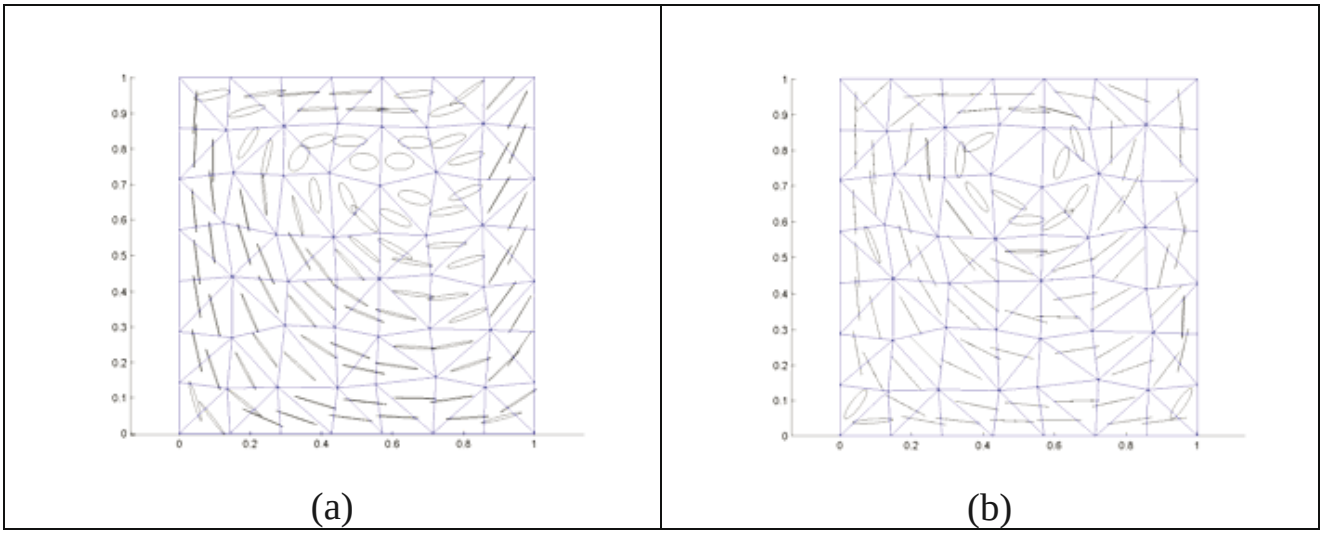

Figure 1. *Steady Fiber orientation distribution in a lid-driven cavity: (a) solution involving a quadratic closure relation (b) Fokker-Planck solution*

Thus, it seems that the use of the Fokker-Planck equation is better when very accurate solutions are searched. However, this equation is multidimensional due to the dependence of the orientation distribution on the physical and conformation variables. Some tentative for solving this equation exist in the bibliography: (i) the use of particles or smoothed particles in a meshless framework (Chinesta et al., 2003; Chiba et al., 1998; Chaubal et al., 1997; …), the use of different polynomial basis (wavelets, orthogonal polynomials, …) or the use of hybrid approximations

(polynomials and particles) in the context of an operator splitting of the Fokker-Planck advection-diffusion equation.

However, in all the cases, a lot of polynomials or particles are introduced in the approximation despite that their contribution in the final solution can be sometimes negligible. In this work we propose a new approximation, efficient and accurate, based on the use of an adaptive model reduction which couples the proper orthogonal decomposition (Karhunen-Loève) with an approximation basis enrichment based on the use of the Krylov subspaces (Ryckelynck, 2003).

2. Mechanical model

The mechanical model governing the short fiber suspension (SFS) flow is given by the following equations: (Batchelor, 1970; Batchelor, 1971; Hinch and Leal, 1975; Hinch and Leal, 1976)

- The momentum balance equation, when the inertia and mass terms are neglected, results

$$Div\underline{\underline{\sigma}} = \underline{0} \qquad [1]$$

where $\underline{\underline{\sigma}}$ is the stress tensor.

- The mass balance equation for incompressible fluids

$$Div\underline{v} = 0 \qquad [2]$$

where $\underline{v}$ represents the velocity field.

- The constitutive equation for a dilute suspension of high aspect-ratio particles is given, with other simplifying assumptions (Tucker, 1991), by

$$\underline{\underline{\sigma}} = -p\underline{\underline{I}} + 2\eta\left\{\underline{\underline{D}} + N_p\left(\underline{\underline{a}} : \underline{\underline{D}}\right)\right\} \qquad [3]$$

where p denotes the pressure, $\underline{\underline{I}}$ the unit tensor, η the viscosity which depends on the chosen model as discussed in Meslin and Poitou (1999), $\underline{\underline{D}}$ the strain rate tensor, N_p a scalar parameter depending on both the fiber concentration and the fiber aspect ratio, ":" the tensorial product twice

contracted (i.e. $\left(\underline{\underline{\underline{\underline{a}}}} : \underline{\underline{D}}\right)_{ij} = a_{ijkl} D_{kl}$) and $\underline{\underline{\underline{\underline{a}}}}$ the fourth order orientation tensor defined by

$$\underline{\underline{\underline{\underline{a}}}} = \int \underline{\rho} \otimes \underline{\rho} \otimes \underline{\rho} \otimes \underline{\rho}\, \psi(\underline{\rho})\, d\underline{\rho} \qquad [4]$$

where $\underline{\rho}$ is the unit vector aligned in the fiber axis direction, "$\otimes$" denotes the tensorial product (i.e. $\left(\underline{\rho} \otimes \underline{\rho}\right)_{ij} = \rho_i \rho_j$), and $\psi(\underline{\rho})$ is the orientation distribution function satisfying the normality condition

$$\int \psi(\underline{\rho})\, d\underline{\rho} = 1 \qquad [5]$$

If $\psi\left(\underline{\rho}\right) = \delta\left(\underline{\rho} - \hat{\underline{\rho}}\right)$, with $\delta(\,)$ the Dirac's distribution, all the orientation probability is concentrated in the direction defined by $\hat{\underline{\rho}}$, and the corresponding orientation tensor results $\underline{\underline{\underline{\underline{\hat{a}}}}} = \hat{\underline{\rho}} \otimes \hat{\underline{\rho}} \otimes \hat{\underline{\rho}} \otimes \hat{\underline{\rho}}$.

We can also define the second order orientation tensor as

$$\underline{\underline{a}} = \int \underline{\rho} \otimes \underline{\rho}\, \psi(\underline{\rho})\, d\underline{\rho} \qquad [6]$$

It is easy to verify that if $\psi(\underline{\rho}) = \delta(\underline{\rho} - \hat{\underline{\rho}})$, the fourth order orientation tensor can be written as

$$\underline{\underline{\underline{\underline{a}}}} = \underline{\underline{a}} \otimes \underline{\underline{a}} \qquad [7]$$

whose components are defined by $a_{ijkl} = a_{ij} a_{kl}$.

For general expressions of $\psi(\underline{\rho})$ the previous relation is not exact and equation [7] becomes a closure approximation known as the quadratic closure relation. However, other closure relations are usually applied (Advani and Tucker, 1990; Dupret et al., 1998), among them we can consider the linear closure relation

$$a_{ijkl} = -\frac{1}{24}(\delta_{ij}\delta_{kl} + \delta_{ik}\delta_{jl} + \delta_{il}\delta_{jk}) + \frac{1}{6}(a_{ij}\delta_{kl} + a_{ik}\delta_{jl} + a_{il}\delta_{jk} + a_{kl}\delta_{ij} + a_{jl}\delta_{ik} + a_{jk}\delta_{il}) \qquad [8]$$

the hybrid closure relation

$$a_{ijkl} = f a_{ij} a_{kl} + (1-f)\left(\begin{array}{l} -\frac{1}{24}(\delta_{ij}\delta_{kl} + \delta_{ik}\delta_{jl} + \delta_{il}\delta_{jk}) + \\ +\frac{1}{6}(a_{ij}\delta_{kl} + a_{ik}\delta_{jl} + a_{il}\delta_{jk} + \\ \qquad + a_{kl}\delta_{ij} + a_{jl}\delta_{ik} + a_{jk}\delta_{il}) \end{array} \right) \qquad [9]$$

where $f = 1 - 4\det(\underline{\underline{a}})$ -en 2D-; and finally, the natural closure relation (Dupret et al., 1998)

$$a_{ijkl} = \frac{1}{6}\det(\underline{\underline{a}})(\delta_{ij}\delta_{kl} + \delta_{ik}\delta_{jl} + \delta_{il}\delta_{jk}) + \frac{1}{3}(a_{ij}a_{kl} + a_{ik}a_{jl} + a_{il}a_{jk}) \qquad [10]$$

The main limitation in using the evolution equations governing the evolution of the different orientation tensors is due to the necessity of introducing a closure relation, whose incidence on the computed results may be significant.

The isotropic orientation state in 2D is defined by the uniform distribution function

$$\Psi = \frac{1}{2\pi} \qquad [11]$$

and then, the second order orientation tensor related to that isotropic orientation state is

$$\underline{\underline{a}} = \frac{\underline{\underline{I}}}{2} \qquad [12]$$

It is easy to verify that for uniform orientation distributions (2D or 3D) the linear closure becomes exact.

From a physical point of view, we can consider that the eigenvalues of the second order orientation tensor represent the probability of finding the fiber in the direction of the corresponding eigenvectors.

If we consider spheroidal fibers immersed in a dilute suspension, we can describe the orientation evolution by means of the Jeffery equation (Jeffery, 1922)

$$\frac{d\underline{\rho}}{dt} = \underline{\underline{\Omega}}\,\underline{\rho} + k\left(\underline{\underline{D}}\,\underline{\rho} - \left(\underline{\underline{D}} : \left(\underline{\rho} \otimes \underline{\rho}\right)\right)\underline{\rho} \right) \qquad [13]$$

where $\underline{\underline{\Omega}}$ is the vorticity tensor, k is a constant that depends on the fiber aspect ratio r (fiber length to fiber diameter ratio)

$$k = \left(r^2 - 1\right) / \left(r^2 + 1\right) \qquad [14]$$

On the other hand the evolution of the fiber orientation distribution ψ is governed by the Fokker-Planck equation,

$$\frac{d\psi(\underline{\rho})}{dt} + \frac{\partial}{\partial \underline{\rho}} \left\{ \psi(\underline{\rho}) \frac{d\underline{\rho}}{dt} \right\} = 0 \qquad [15]$$

where the material derivative is given by

$$\frac{d\psi}{dt} = \frac{\partial \psi}{\partial t} + \underline{v}\, Grad\psi \qquad [16]$$

Now, taking into account equations [6], [13] and [15], the equation that governs the evolution of the second order orientation tensor can be deduced

$$\frac{d\,\underline{\underline{a}}}{dt} = \underline{\underline{\Omega}}\,\underline{\underline{a}} - \underline{\underline{a}}\,\underline{\underline{\Omega}} + k\left(\underline{\underline{D}}\,\underline{\underline{a}} + \underline{\underline{a}}\,\underline{\underline{D}} - 2\left(\underline{\underline{\underline{a}}} : \underline{\underline{D}} \right) \right) \qquad [17]$$

A similar equation can be derived for the evolution of the fourth order orientation tensor, which in this case involves the sixth-order orientation tensor. To take account of fiber interaction effects in semi-concentrated suspensions Folgar and Tucker (1984) proposed the introduction of a diffusion term in the Fokker-Planck equation, i.e.

$$\frac{d\psi(\underline{\rho})}{dt} + \frac{\partial}{\partial \underline{\rho}} \left\{ \psi(\underline{\rho}) \frac{d\underline{\rho}}{dt} \right\} = \frac{\partial}{\partial \underline{\rho}} \left\{ D_r \frac{\partial \psi(\underline{\rho})}{\partial \underline{\rho}} \right\} \qquad [18]$$

Fiber interaction being taken into account, the equation governing the evolution of $\underline{\underline{a}}$ then yields

$$\frac{d\,\underline{\underline{a}}}{dt} = \underline{\underline{\Omega}}\,\underline{\underline{a}} - \underline{\underline{a}}\,\underline{\underline{\Omega}} + k\left(\underline{\underline{D}}\,\underline{\underline{a}} + \underline{\underline{a}}\,\underline{\underline{D}} - 2\left(\underline{\underline{\underline{a}}} : \underline{\underline{D}} \right) \right) - 4D_r \left(\underline{\underline{a}} - \frac{\underline{\underline{I}}}{N} \right) \qquad [19]$$

$$N = \begin{cases} 2 & \text{in } 2D \\ 3 & \text{in } 3D \end{cases} \qquad [20]$$

3. The alpha-Natural Element Method

In the last decade considerable research efforts have been paid to the development of a series of novel numerical tools that have been referred as meshless or meshfree methods. These methods do not need explicit connectivity information, as required in standard FEM. The geometrical information is generated in a process transparent to the user, alleviating the pre-processing stage of the method. They also present outstanding advantages in modelling complex phenomena, such as large deformation problems, forming processes, fluid flow, etc, where traditional and more experienced techniques, like the FEM, fail due to the need of excessive remeshing.

The Natural Element Method (NEM) is one of the latest meshless technique applied in the field of linear elastostatics. It has unique features among meshless Galerkin methods, such as interpolant character of shape functions and exact application of essential boundary conditions (see the review paper from Cueto et al., 2003). In addition to its inherent meshless structure, these capabilities make the NEM an appealing choice also for application in the simulation of fluid flows. The NEM is based on the natural neighbour interpolation scheme, which in turn relies on the concepts of Voronoi diagrams and Delaunay triangulations (see figure 2a), to build Galerkin trial and test functions. These are defined as the *natural neighbour* coordinates (also known as Sibson's coordinates) of the point under consideration, that is, with respect to figure 2b, the value at point $\underline{x}$ of the shape function associated with the node 1, is defined by:

$$\phi_1(\underline{x}) = \frac{Area(abfe)}{Area(abcd)} \qquad [21]$$

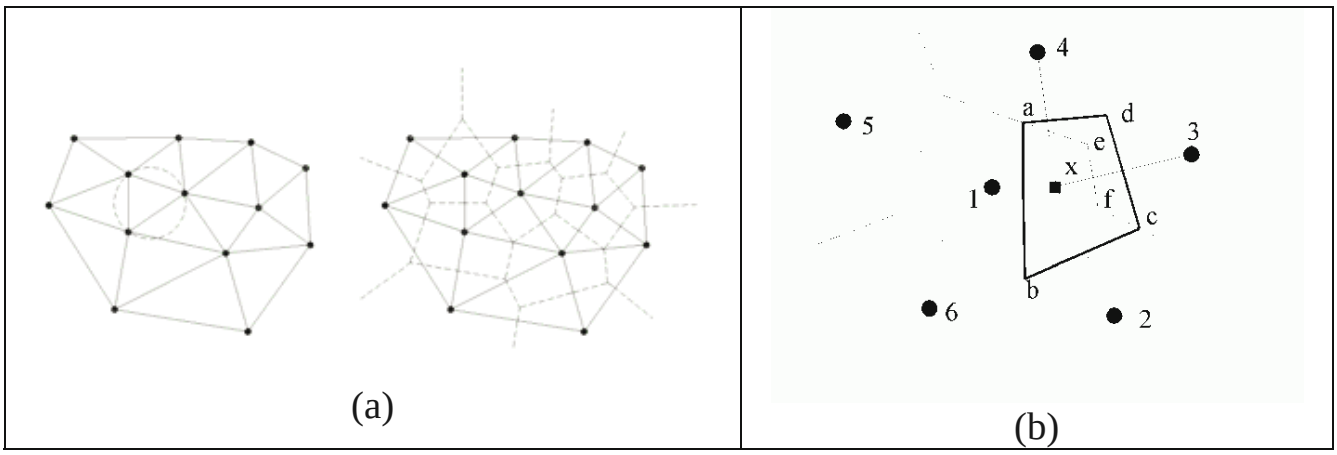

Figure 2. (a) *Delaunay and Voronoi diagrams,* (*b*) *Natural neighbour interpolants*

These functions are used to build the discrete system of equations arising from the application of the Galerkin method in the usual way. It has been proved, that the angles of the Delaunay triangles are not influencing the quality of the results, in opposition to the FEM. In addition, the NEM has interesting properties such as

linear consistency and smoothness of the shape functions (natural neighbour coordinates are C^1 everywhere except at the nodes, where they are C^0). But perhaps the most interesting property of the Natural Element Method is the Kronecker delta property, i.e. $\phi_i(x_j)=\delta_{ij}$. In opposition to the vast majority of meshless methods, the NEM shape functions are strictly interpolants. This property allows an exact reproduction of linear (even bilinear in some 3D cases) displacement fields on the boundary of convex domains, since the influence of interior points vanishes along convex boundaries. This is not true in non-convex ones, where some specific treatment is required. The alpha-shape concept allows to circumvent this difficulty when it is used in the context of a natural neighbour interpolation (Cueto et al., 2003).

The application of the NEM for complex fluid flow simulations has been recently proposed in Martinez et al. (2003). The main advantage of using the NEM in the framework of an updated Lagrangian formulation for simulating free or moving surface flows is the fact that the nodal position can be updated from the flow kinematics, without remeshing requirements, allowing the accurate description of large transformations and the history effects.

4. Coupling the alpha-NEM with a particle approach of the Fokker-Planck equation

The use of the natural element method allows an accurate and robust approximation of the fields involved in the weak form of the motion equations when the anisotropic viscosity is assumed to be known (computed at the previous step when an explicit algorithm or a fixed point scheme in the implicit case is used). In order to approach to the verification of the LBB condition two possibilities exist: (i) the use of a natural neighbor interpolation for the velocity field and a discontinuous pressure approximation, that despite the fact that it does not verify the LBB condition, no locking problems have been noticed, or (ii) the use of mixed approximations verifying the LBB condition, that can be constructed for example in the framework of the partition of unity (Cueto et al. 2004). More details concerning this approach, when it is combined with the integration of the advection equation governing the evolution of the second order orientation tensor, can be found in Martinez et al. (2003).

In order to couple the alpha-NEM with a particle strategy for solving the Fokker-Planck equation, we assume at each node at the initial time a set of N particles (virtual fibers) with the orientations (for the sake of simplicity only the 2D case is considered in this paper) defined by the angle θ respect to the x-axis:

$$\theta_i = i \times \frac{2\pi}{N}, \quad i \in [0, \cdots, N-1] \qquad [22]$$

Thus, the center of mass of each one of these *N* fibers is moving with the fluid, and at each time they are located on the considered "material" node. Of course, the orientation of these fibers evolves in time according to the Jeffery's equation [13].

In the 2D case the unit vector describing the orientation of each particle can be expressed by

$$\underline{\rho} = \begin{pmatrix} \cos\theta \\ \sin\theta \end{pmatrix} \qquad [23]$$

that introduced in the Jeffery's equation results in

$$\dot{\theta}\begin{pmatrix} -\sin\theta \\ \cos\theta \end{pmatrix} = \begin{pmatrix} 0 & \frac{1}{2}\left(\frac{\partial u}{\partial y}+\frac{\partial v}{\partial x}\right) \\ -\frac{1}{2}\left(\frac{\partial u}{\partial y}+\frac{\partial v}{\partial x}\right) & 0 \end{pmatrix}\begin{pmatrix} \cos\theta \\ \sin\theta \end{pmatrix} + k\begin{pmatrix} \frac{\partial u}{\partial x} & \frac{1}{2}\left(\frac{\partial u}{\partial y}+\frac{\partial v}{\partial x}\right) \\ \frac{1}{2}\left(\frac{\partial u}{\partial y}+\frac{\partial v}{\partial x}\right) & \frac{\partial v}{\partial y} \end{pmatrix}\begin{pmatrix} \cos\theta \\ \sin\theta \end{pmatrix} -$$

$$-k\left[\begin{pmatrix} \cos\theta & \sin\theta \end{pmatrix}\begin{pmatrix} \frac{\partial u}{\partial x} & \frac{1}{2}\left(\frac{\partial u}{\partial y}+\frac{\partial v}{\partial x}\right) \\ \frac{1}{2}\left(\frac{\partial u}{\partial y}+\frac{\partial v}{\partial x}\right) & \frac{\partial v}{\partial y} \end{pmatrix}\begin{pmatrix} \cos\theta \\ \sin\theta \end{pmatrix}\right]\begin{pmatrix} \cos\theta \\ \sin\theta \end{pmatrix}$$

that pre-multiplying by $\begin{pmatrix} -\sin\theta & \cos\theta \end{pmatrix}$ gives the expresion of the fiber rotation velocity

$$\dot{\theta} = \begin{pmatrix} -\sin\theta & \cos\theta \end{pmatrix}\begin{pmatrix} 0 & \frac{1}{2}\left(\frac{\partial u}{\partial y}+\frac{\partial v}{\partial x}\right) \\ -\frac{1}{2}\left(\frac{\partial u}{\partial y}+\frac{\partial v}{\partial x}\right) & 0 \end{pmatrix}\begin{pmatrix} \cos\theta \\ \sin\theta \end{pmatrix} +$$

$$+k\begin{pmatrix} -\sin\theta & \cos\theta \end{pmatrix}\begin{pmatrix} \frac{\partial u}{\partial x} & \frac{1}{2}\left(\frac{\partial u}{\partial y}+\frac{\partial v}{\partial x}\right) \\ \frac{1}{2}\left(\frac{\partial u}{\partial y}+\frac{\partial v}{\partial x}\right) & \frac{\partial v}{\partial y} \end{pmatrix}\begin{pmatrix} \cos\theta \\ \sin\theta \end{pmatrix} \qquad [24]$$

Thus, the dependence of the rotation velocity on: (i) the fiber orientation θ; (ii) the gradient of velocities and (iii) the fiber aspect ratio, becomes explicit in equation [24], and by simplicity we indicate these dependencies by

$$\dot{\theta} = \dot{\theta}\left(Grad\,\underline{v}, k, \theta\right) \qquad [25]$$

The algoritm can be written in the form

- For each time step *n*
  - For each node *k*
    - Compute the gradient of velocity at that node from the velocity field computed at the previous step:
      $Grad\,\underline{v}^{n-1}\Big|_{\underline{x}_k^{n-1}}$
    - Update the particle position: $\underline{x}_k^n = \underline{x}_k^{n-1} + \underline{v}_k^{n-1}\Delta t$
    - For each one of the N fibers associated with the node *k*:
      - Compute the rotation velocity:
        $$\dot{\theta}_{i,k}^{n-1} = \dot{\theta}_{i,k}^{n-1}\left(Grad\,\underline{v}^{n-1}\Big|_{\underline{x}_k^{n-1}}, k, \theta_{i,k}^{n-1}\right)$$
      - Update its orientation:
        $$\theta_{i,k}^n = \theta_{i,k}^{n-1} + \dot{\theta}_{i,k}^{n-1}\,\Delta t$$
    - Compute the components of the fourth order orientation tensor at that node *k:* $\underline{\underline{\underline{\underline{a}}}}_k^n = \int \underline{\rho}\otimes\underline{\rho}\otimes\underline{\rho}\otimes\underline{\rho}\,\psi_k^n\,d\underline{\rho}$,

      with $\psi_k^n(\theta) = \sum_{\mathrm{i=0}}^{\mathrm{i=N\text{-}1}} \frac{1}{N}\delta\left(\theta - \theta_{i,k}^n\right)$, being its discrete form:

$$\begin{cases} a_{1111,k}^n = \sum_{i=0}^{i=N-1} \cos^4\theta_{i,k}^n \,\frac{1}{N} \\ a_{1112,k}^n = \sum_{i=0}^{i=N-1} \cos^3\theta_{i,k}^n \sin\theta_{i,k}^n \,\frac{1}{N} \\ a_{1122,k}^n = \sum_{i=0}^{i=N-1} \cos^2\theta_{i,k}^n \sin^2\theta_{i,k}^n \,\frac{1}{N} \\ a_{1222,k}^n = \sum_{i=0}^{i=N-1} \cos\theta_{i,k}^n \sin^3\theta_{i,k}^n \,\frac{1}{N} \\ a_{2222,k}^n = \sum_{i=0}^{i=N-1} \sin^4\theta_{i,k}^n \,\frac{1}{N} \end{cases}$$

      verifying the symmetry relations:

      $a_{1112} = a_{1121} = a_{1211} = a_{2111}$;

      $a_{1122} = a_{1221} = a_{2211} = a_{2112} = a_{1212} = a_{2121}$; ...

  - With the fourth-order orientation tensor just computed at each node, we can proceed to update the flow kinematics by solving the anisotropic Stokes problem in the framework of an alpha-NEM

discretisation. The only new term related to the fiber presence in the flow kinematics variational formulation is:

$$\underline{\underline{\underline{a}}} : \underline{\underline{D}} = a_{ijkl} D_{kl} = a_{ij11} D_{11} + a_{ij12} D_{12} + a_{ij21} D_{21} + a_{ij22} D_{22}$$

$$\begin{aligned}\underline{\underline{D}}^* : \left(\underline{\underline{\underline{a}}} : \underline{\underline{D}} \right) &= D_{11}^* \left(a_{1111} D_{11} + a_{1112} D_{12} + a_{1121} D_{21} + a_{1122} D_{22} \right) + \\ &+ D_{12}^* \left(a_{1211} D_{11} + a_{1212} D_{12} + a_{1221} D_{21} + a_{1222} D_{22} \right) + \\ &+ D_{21}^* \left(a_{2111} D_{11} + a_{2112} D_{12} + a_{2121} D_{21} + a_{2122} D_{22} \right) + \\ &+ D_{22}^* \left(a_{2211} D_{11} + a_{2212} D_{12} + a_{2221} D_{21} + a_{2222} D_{22} \right) = \end{aligned}$$

$$\begin{pmatrix} D_{11}^* & D_{12}^* & D_{21}^* & D_{22}^* \end{pmatrix} \begin{pmatrix} a_{1111} & a_{1112} & a_{1121} & a_{1122} \\ a_{1211} & a_{1212} & a_{1221} & a_{1222} \\ a_{2111} & a_{2112} & a_{2121} & a_{2122} \\ a_{2211} & a_{2212} & a_{2221} & a_{2222} \end{pmatrix} \begin{pmatrix} D_{11} \\ D_{12} \\ D_{21} \\ D_{22} \end{pmatrix} = \left(\underline{D}^* \right)^T \underline{\underline{A}} \underline{D}$$

resulting the extra-stress term: $\int_\Omega \left(\underline{D}^* \right)^T \left[2\eta \underline{\underline{I}} + 2\eta N_p \underline{\underline{A}} \right] \underline{D} d\Omega$

Figure 3 depicts at the 19th time step of a suspension flow simulation in an extrusion die ($\Delta t = 0.007 s., N_p = 10, \mathrm{k} = 0.8$): (a) the velocity field and (b) the fiber orientation, when an isotropic fiber orientation is assumed at the initial time. In this representation the ellipses axes represents the principal orientation directions, being their lengths proportional to the orientation intensity. These axes and their length have been obtained as the eigenvectors and eigenvalues related to the second order orientation tensor which is computed at each node using the following relations:

$$\begin{cases} a_{11,k}^n = \sum_{i=0}^{i=N-1} \cos^2 \theta_{i,k}^n \, \frac{1}{N} \\ a_{12,k}^n = \sum_{i=0}^{i=N-1} \cos \theta_{i,k}^n \sin \theta_{i,k}^n \, \frac{1}{N} \\ a_{21,k}^n = a_{12,k}^n \\ a_{22,k}^n = \sum_{i=0}^{i=N-1} \sin^2 \theta_{i,k}^n \, \frac{1}{N} \end{cases}$$

In a former paper (see Martinez et al., 2003), the coupling between the alpha-NEM and an integration by characteristics of the equation governing the evolution of the second order orientation tensor was considered, in the context of a similar scheme, where the evolution equation was integrated along the nodal trajectories.

When the diffusion effects are accounted, we can proceed in a stochastic manner, adding a random rotation term to the purely advective Jeffery rotation.

However, in this case we need to increase the number of fibers involved in the computation. In fact, we have proved in Chinesta et al. (2003) that at each angle we need to consider a lot of number of fibers, which makes inefficient this kind of simulation. The other possibility lies in the definition of an advective rotation velocity which takes into account the diffusion effects in the context of a smooth particle approximation, as described in Ammar and Chinesta (2004).

The main drawback of these kind of approximations is the large number of functions or particles involved in the computation, despite the fact that sometimes they are not relevant in the searched solution. The problem of the model reduction is then addressed.

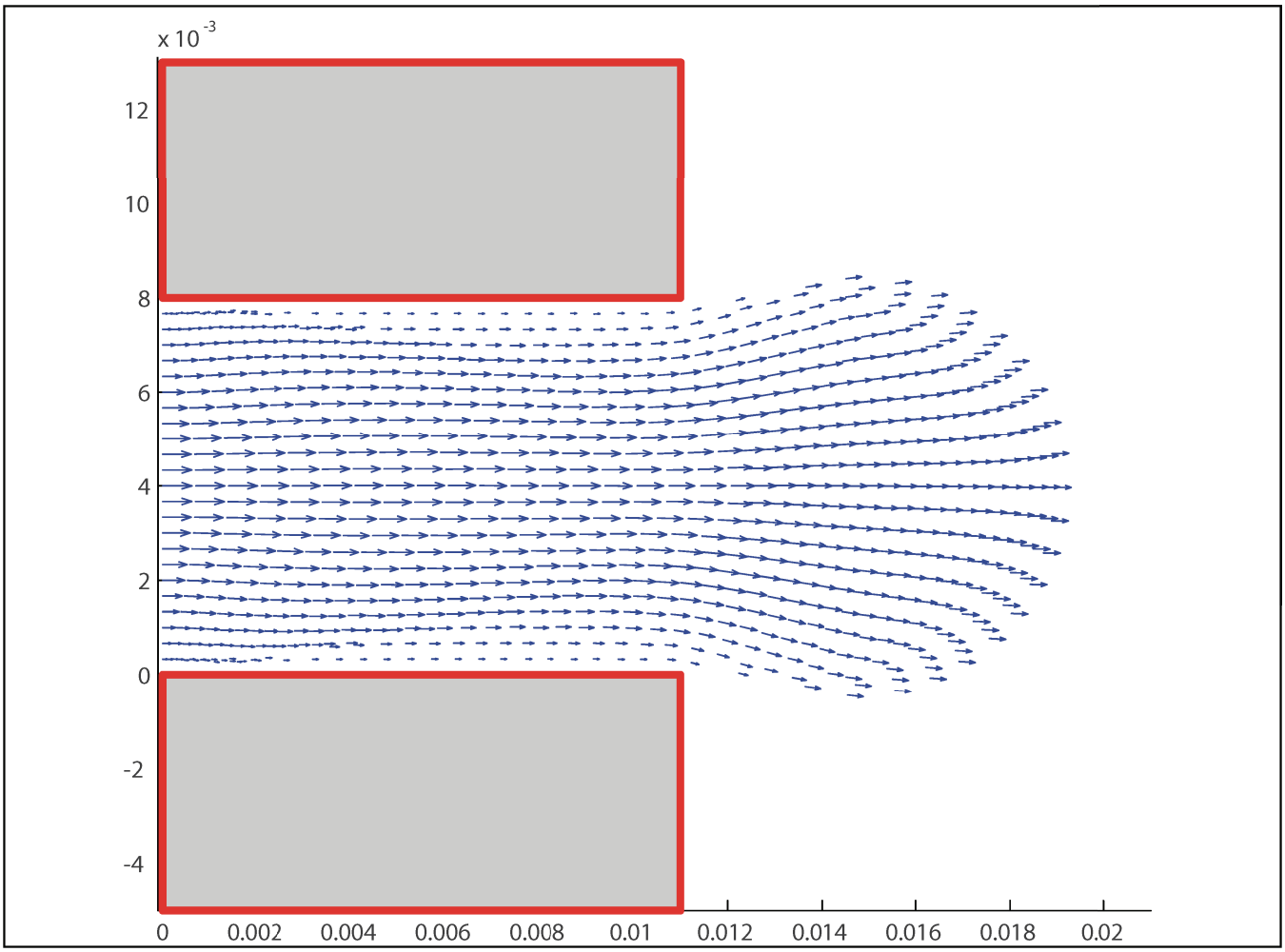

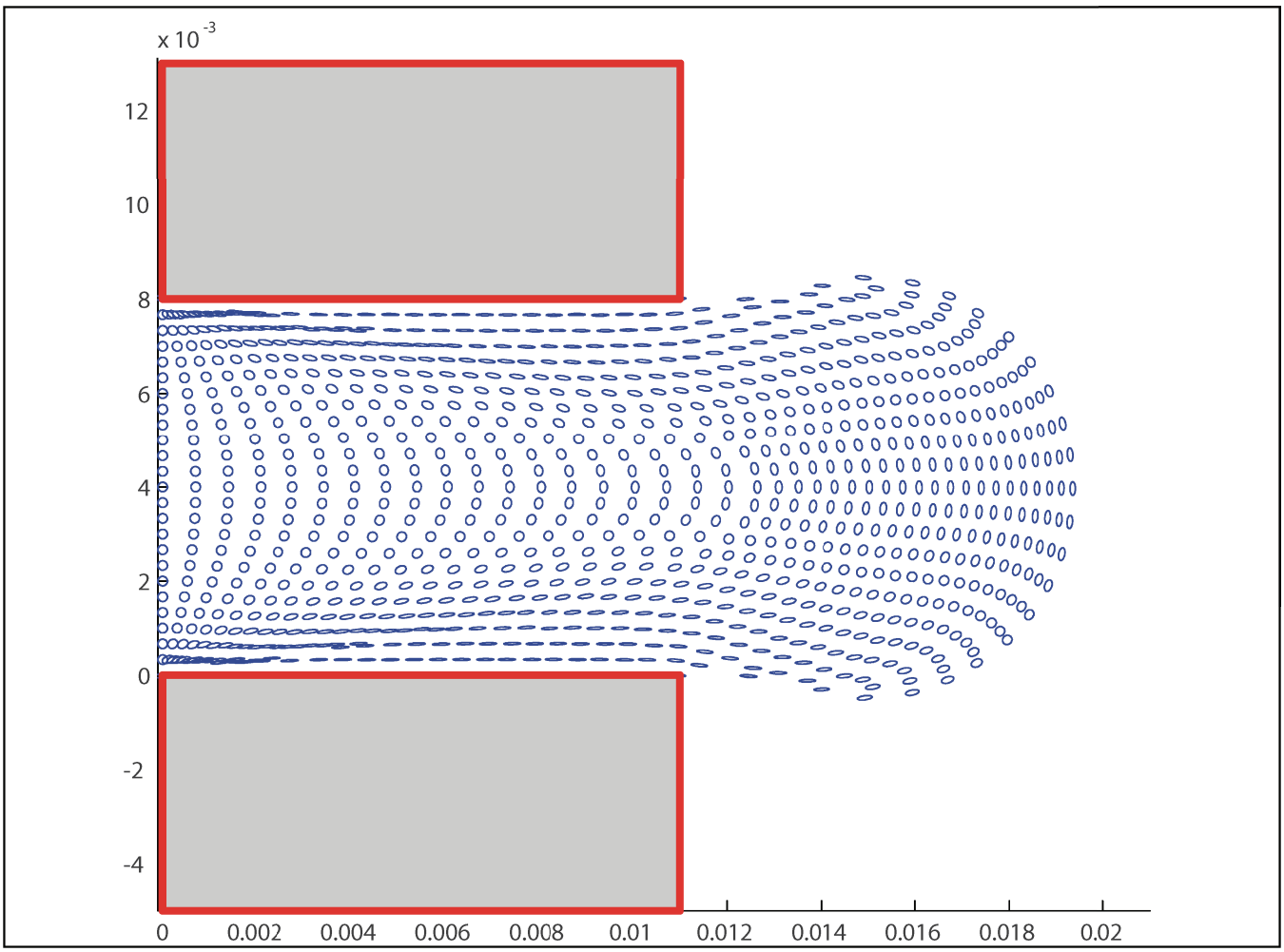

Figure 3. Extrusion flow simulation: (a) velocity field and (b) fiber orientation.

5. Reduced order modeling

As just commented, some 2D or 3D problems remain today untreatable because the extremely large number of degrees of freedom –*dof*- involved. To alleviate this drawback, one possibility lies in the use of a model reduction (based on the Karhunen-Loève decomposition –KLD-, also known as proper orthogonal decomposition –POD-). Model reduction techniques have been successfully applied in the finite element framework for modelling dynamic models of distributed parameters (Park and Cho, 1996). However, in these applications several direct problems must be solved to extract empirical functions that represent the system most efficiently. This set of empirical eigenfunctions is used as functional basis of the Galerkin procedure to lump the governing equation. Thus, for example, the resulting lumped parameter model can be used to obtain the solution when the boundary conditions are changing randomly. To avoid, these preliminary costly calculations, Ryckelynck proposed (Ryckelynck, 2003) to start the resolution process from any reduced basis, using the Krylov subspaces generated by the governing equation residual for enriching the approximation basis, at the same time that a proper orthogonal decomposition extracts relevant information in order to maintain the low order of the approximation basis. Moreover, he has proved that

there is an appropriate choice of a reduced number of weighting function able to solve the problem efficiently. He has called this technique “A priori model hyper-reduction”, (Ryckelynck, 2004) but this approach in not concerned in the present work.

5.1. *The Karhunen-Loève decomposition*

We assume that the evolution of a certain field is known $u(\underline{x},t)$. In practical applications, this field is expressed in a discrete form, that is, it is known at the nodes of a spatial mesh and for some times $u(\underline{x}_i,t^p)\equiv u_i^p$. We can also write introducing a spatial interpolation $u^p(\underline{x})\equiv u(\underline{x},t=p\Delta t);\forall p\in[1,\cdots,P]$. The main idea of the Karhunen-Loève (KL) decomposition is how to obtain the most typical or characteristic structure $\phi(\underline{x})$ among these $u^p(\underline{x}),\forall p$. This is equivalent to obtaining a function $\phi(\underline{x})$ that minimizes α

$$\alpha=\sum_{p=1}^{p=P}\left[\sum_{i=1}^{i=N}\left(u^p(\underline{x}_i)-\phi(\underline{x}_i)\right)^2\right] \qquad [26]$$

that is equivalent to maximize α defined by

$$\alpha=\frac{\frac{1}{P}\sum_{p=1}^{p=P}\left[\sum_{i=1}^{i=N}\phi(\underline{x}_i)u^p(\underline{x}_i)\right]^2}{\sum_{i=1}^{i=N}\left(\phi(\underline{x}_i)\right)^2} \qquad [27]$$

The maximisation leads to:

$$\frac{1}{P}\sum_{p=1}^{p=P}\left[\left[\sum_{i=1}^{i=N}\tilde{\phi}(\underline{x}_i)u^p(\underline{x}_i)\right]\left[\sum_{j=1}^{j=N}\phi(\underline{x}_j)u^p(\underline{x}_j)\right]\right]=\alpha\sum_{i=1}^{i=N}\tilde{\phi}(\underline{x}_i)\phi(\underline{x}_i);\ \forall\tilde{\phi} \qquad [28]$$

which can be rewritten in the form

$$\sum_{i=1}^{i=N}\left[\sum_{j=1}^{j=N}\left\{\frac{1}{P}\sum_{p=1}^{p=P}u^p(\underline{x}_i)u^p(\underline{x}_j)\phi(\underline{x}_j)\right\}\tilde{\phi}(\underline{x}_i)\right]=\alpha\sum_{i=1}^{i=N}\tilde{\phi}(\underline{x}_i)\phi(\underline{x}_i);\quad \forall\tilde{\phi} \qquad [29]$$

Defining the vectors $\underline{a}$ such that its i-component is $a(\underline{x}_i)$, Eq. [29] takes the following matrix form

$$\underline{\tilde{\phi}}^T \underline{\underline{k}}\, \underline{\phi} = \alpha\, \underline{\tilde{\phi}}^T \underline{\phi};\ \ \forall \underline{\tilde{\phi}} \ \ \Rightarrow\ \ \underline{\underline{k}}\, \underline{\phi} = \alpha \underline{\phi} \qquad [30]$$

where the two points correlation matrix is given by

$$k_{ij} = \frac{1}{P}\sum_{p=1}^{p=P} u^p\left(\underline{x}_i\right) u^p\left(\underline{x}_j\right) \Leftrightarrow \underline{\underline{k}} = \frac{1}{P}\sum_{p=1}^{p=P} \underline{u}^p \left(\underline{u}^p\right)^T \qquad [31]$$

which is symmetric and positive definite. If we define the matrix $\underline{\underline{Q}}$ containing the discrete field history:

$$\underline{\underline{Q}} = \begin{pmatrix} u_1^1 & u_1^2 & \cdots & u_1^P \\ u_2^1 & u_2^2 & \cdots & u_2^P \\ \vdots & \vdots & \ddots & \vdots \\ u_N^1 & u_N^2 & \cdots & u_N^P \end{pmatrix} \qquad [32]$$

is easy to verify that the matrix $\underline{\underline{k}}$ in Eq. [31] results

$$\underline{\underline{k}} = \underline{\underline{Q}}\, \underline{\underline{Q}}^T \qquad [33]$$

where the diagonal components are given by

$$\underline{\underline{k}}_{ii} = \left(\underline{\underline{Q}}\, \underline{\underline{Q}}^T\right)_{ii} = \sum_{j=1}^{j=P} \left(u_i^j\right)^2 \qquad [34]$$

In the same way we have

$$\underline{\underline{M}} = \underline{\underline{k}}^T = \underline{\underline{Q}}^{\mathrm{T}}\, \underline{\underline{Q}} \qquad [35]$$

whose eigenvectors $\underline{\psi}$ are of dimension *P*, and they depend on the time:

$$\underline{\underline{M}}\ \underline{\psi} = \lambda\, \underline{\psi} \qquad [36]$$

The relation between the eigenvectors $\underline{\phi}_k$ and $\underline{\psi}_k$ is

$$\underline{\phi}_k = \underline{\underline{Q}}\, \underline{\psi}_k \frac{1}{\sqrt{\alpha_k}} \qquad [37]$$

relation which derives from

$$\underline{\underline{k}}\,\underline{\phi} = \alpha\,\underline{\phi} \Rightarrow \underline{\underline{Q}}\,\underline{\underline{Q}}^T\,\underline{\phi}_k = \alpha_k\,\underline{\phi}_k \qquad [38]$$

and from Eq. [36]

$$\underline{\underline{M}}\,\underline{\psi}_k = \underline{\underline{Q}}^T\,\underline{\underline{Q}}\,\underline{\psi}_k = \lambda_k\,\underline{\psi}_k \Rightarrow \underline{\underline{Q}}\,\underline{\underline{Q}}^T\,\underline{\underline{Q}}\,\underline{\psi}_k = \lambda_k\,\underline{\underline{Q}}\,\underline{\psi}_k \qquad [39]$$

The previous relations implies

$$\underline{\phi}_k = \frac{\underline{\underline{Q}}\,\underline{\psi}_k}{\left\|\underline{\underline{Q}}\,\underline{\psi}_k\right\|} \qquad [40]$$

being $\alpha_k = \lambda_k$. Eq. [37] is obtained accounting that

$$\underline{\underline{Q}}^T\,\underline{\underline{Q}}\,\underline{\psi}_k = \lambda_k\,\underline{\psi}_k \Rightarrow \underline{\psi}_k^T\,\underline{\underline{Q}}^T\,\underline{\underline{Q}}\,\underline{\psi}_k = \left\|\underline{\underline{Q}}\,\underline{\psi}_k\right\|^2 = \lambda_k\,\underline{\psi}_k^T\,\underline{\psi}_k = \lambda_k \qquad [41]$$

Thus, the functions defining the most characteristic structure of $u^p(\underline{x})$ are the eigenfunctions $\phi_k(\underline{x}) \equiv \underline{\phi}_k$ associated with the highest eigenvalues.

5.2 *"A posteriori" reduced modeling*

If some direct simulations are carried out, we can determine $u(\underline{x}_i, t^p) \equiv u_i^p, \forall i \in [1,\cdots,N], \forall p \in [1,\cdots,P]$, and from these the n eigenvectors related to the n-highest eigenvalues $\underline{\phi}_k = \phi_k(\underline{x}_i), \forall i \in [1,\cdots,N], \forall k \in [1,\cdots,n]$. Now, we can try to use these n eigenfunctions for approximating the solution of a problem slightly different to the one that has served to define $u(\underline{x}_i, t^p) \equiv u_i^p$. For this purpose we need to define the matrix $\underline{\underline{B}}$

$$\underline{\underline{B}} = \begin{pmatrix} \phi_1(\underline{x}_1) & \phi_2(\underline{x}_1) & \cdots & \phi_n(\underline{x}_1) \\ \phi_1(\underline{x}_2) & \phi_2(\underline{x}_2) & \cdots & \phi_n(\underline{x}_2) \\ \vdots & \vdots & \ddots & \vdots \\ \phi_1(\underline{x}_N) & \phi_2(\underline{x}_N) & \cdots & \phi_n(\underline{x}_N) \end{pmatrix} \qquad [42]$$

Now, if we consider the system of equations resulting from the discretization in the form

$$\underline{\underline{A}}\,\underline{U} = \underline{F} \qquad [43]$$

then, assuming that the unknown vector contains the nodal degrees of freedom, it can be expressed as

$$\underline{U} = \sum_{i=1}^{i=n} \zeta_i \underline{\phi}_i = \underline{\underline{B}}\,\underline{\zeta} \qquad [44]$$

it results

$$\underline{\underline{A}}\,\underline{U} = \underline{F} \Rightarrow \underline{\underline{A}}\,\underline{\underline{B}}\,\underline{\zeta} = \underline{F} \qquad [45]$$

and multiplying both terms by $\underline{\underline{B}}^T$ it results

$$\underline{\underline{B}}^T\,\underline{\underline{A}}\,\underline{\underline{B}}\,\underline{\zeta} = \underline{\underline{B}}^T\,\underline{F} \qquad [46]$$

which proves that the final system of equations is of low order, i.e. the dimensions of $\underline{\underline{B}}^T\,\underline{\underline{A}}\,\underline{\underline{B}}$ are $n \times n$, with $n << N$, and the dimensions of both $\underline{\zeta}$ and $\underline{\underline{B}}^T\,\underline{F}$ are $n \times 1$.

5.3 *Reduced model adaptativity: an "a priori" model reduction approach*

In order to compute reduced model solutions without an "a priori" knowledge, we propose to start with a low order approximation basis, using some simple functions or using the eigenvectors of a "similar" problem. Now, we compute *S* iterations of the evolution problem using the reduced model [46] without changing the approximation basis. After each *S* iterations the complete discrete system [43] is constructed, and the residual $\underline{R}$ evaluated:

$$\underline{R} = \underline{\underline{A}}\,\underline{U} - \underline{F} \qquad [47]$$

If the norm of the residual is small enough, we can continue for other *S* iterations using the same approximation basis. On the contrary, if the residual norm is too large, we need to enrich the approximation basis. This enrichment is built using some Krylov's subspaces $\left\{\underline{R}, \underline{\underline{A}}\,\underline{R}, \underline{\underline{A}}^2\,\underline{R}, \cdots\right\}$, which are added to the most representative information extracted from the previous solutions $\left\{\underline{\zeta}^1, \underline{\zeta}^2, \cdots, \underline{\zeta}^{S-1}\right\}$ as well as from the solutions of "a similar" problem, up to the current step $\left\{\underline{\zeta}^S_{sim}, \underline{\zeta}^{S+1}_{\text{sim}} \cdots\right\}$. The resulting most significant eigenvectors define the matrix $\underline{\underline{\zeta}}$. Then the evolution process is restarted using the enriched basis defined by:

$\left\{\underline{\underline{B}}\,\underline{\zeta}, \underline{R}, \underline{\underline{A}}\,\underline{R}, \underline{\underline{A}}^2\,\underline{R}\right\}$. After each reduced basis modification, both the previous solutions and the ones associated to a "similar problem", are projected into the new basis.

5.4 *Numerical example*

We consider the Fokker-Planck equation [15] governing the 2D evolution of the fiber orientation in a simple shear flow ($\underline{v}^T = (y,0)$) involving a suspension of short fibers with *k=0.2*. When an isotropic initial fiber distribution is considered, i.e. $\psi(t=0) = 1/2\pi$, it evolves in time as depicted in figure 4, where we can notice that fibers align in the flow direction. This solution has been obtained with a finite difference technique using 360 degrees of freedom and an appropriate upwind stabilization of the advection term.

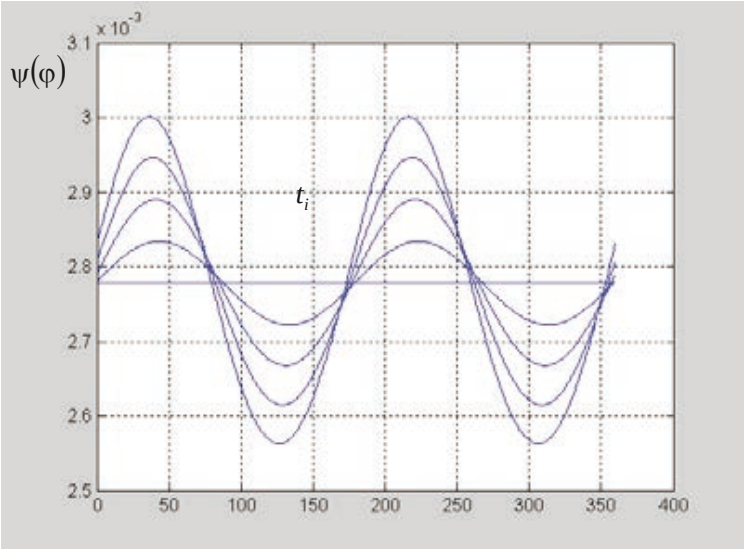

Figure 4. Evolution of the fiber orientation distribution in a simple shear flow.

From this evolution we can extract the most relevant information using the KL decomposition, which results in the four eigenvectors $\psi_n^{k=0.2}(\varphi)$ related to the eigenvalues in the interval $[10^{-8}\lambda_{\max}, \lambda_{\max}]$. These eigenfunctions are depicted in figure 5.

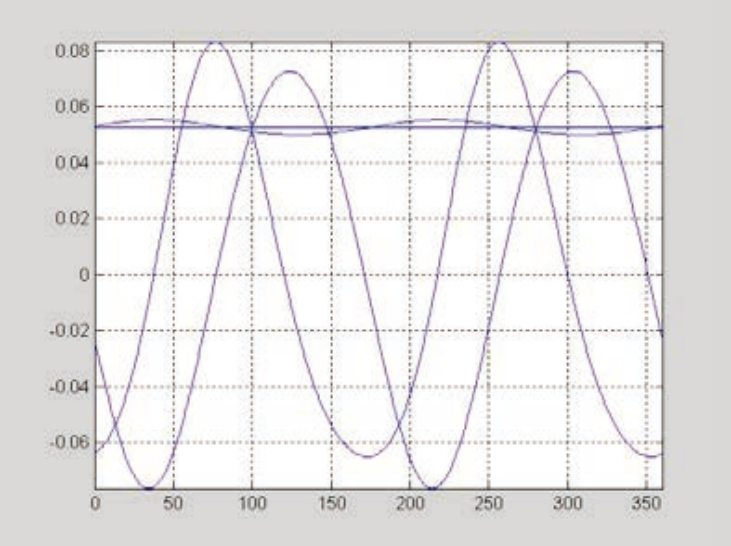

Figure 5. Eigenfunctions related to the evolution shown in figure 4.

Now, we consider the same flow, but for a suspension involving fibers with *k=0.8*, and we compute the fiber orientation evolution using the eigenfunctions previously obtained (for the other fibers aspect ratio). Thus, we write

$$\psi^{red,k=0.8}(\varphi,t)=\sum_{i=1}^{i=4}\beta_i(t)\psi_i^{k=0.2}(\varphi) \qquad [48]$$

that introduced in the 2D Fokker-Planck equation

$$\frac{d\psi}{dt}+\frac{\partial}{\partial\varphi}\left\{\psi(\varphi)\dot{\varphi}\right\}=0 \qquad [49]$$

leads to a linear system of ODE that are integrated using an appropriate finite difference technique, allowing the computation of coefficients $\beta_i(t)$

The reduced order solution obtained at four different times is compared in figure 6 with the reference ones, from which we can notice that a significant deviation appears up to a certain time. Associated with this deviation we can expect a residual, that as previously described, could be used to define the different Krylov's subspaces. To illustrate this enrichment procedure we assume that at a certain time step t_c we control the residual, that is assumed large enough to assure the necessity of a basis enrichment. The beta coefficients at that time are $\beta_i(t_c)$ from which we can compute the solution $\psi^{red,k=0.8}(\varphi,t_c)$ using Eq. [48]. As the previous reduced order solution is also known $\beta_i(t_{c-1})$, whose associated orientation distribution results $\psi^{red,k=0.8}(\varphi,t_{c-1})$, we can compute the time derivative in Eq. [49]:

$$\frac{d\psi}{dt} = \frac{\psi^{red,k=0.8}(\varphi, t_c) - \psi^{red,k=0.8}(\varphi, t_{c-1})}{\Delta t} \qquad [50]$$

The second term in Eq. [49] is evaluated using stabilized finite differences at time t_c with respect to the angular coordinate. In this way the residual is perfectly defined, and taking into account the angular discretization, it can be written in a vector form $\underline{R}(t_c)$. Now, in order to define the other Krylov's subspaces, we need to define the matrix related to the Fokker-Planck evolution problem. From equations [48] and [49] we can write

$$\underline{\underline{A}}\,\dot{\underline{\beta}} + \underline{\underline{D}}\,\underline{\beta} = \underline{0} \qquad [51]$$

where the columns of the matrix $\underline{\underline{A}}$ contain the eigenfunctions $\psi_i^{k=0.2}(\varphi)$, assuming a discretization in the angular coordinate. Thus, the *ij*-component of $\underline{\underline{A}}$ contains the *i*-component of the *j*-eigenvector, i.e. $\psi_j^{k=0.2}(\varphi_i)$. The matrix $\underline{\underline{D}}$ results from the stabilized discretization of the advection operator in Eq. [49]. As both matrix are not square, we proceed to multiply both terms in Eq. [51] by $\underline{\underline{A}}^T$

$$\underline{\underline{A}}^T\,\underline{\underline{A}}\,\dot{\underline{\beta}} + \underline{\underline{A}}^T\,\underline{\underline{D}}\,\underline{\beta} = \underline{0} \qquad [52]$$

that using an implicit temporal discretization, results

$$\underline{\underline{C}}\,\underline{\beta}(t_c) = \underline{\beta}(t_{c-1}) \qquad [53]$$

which leads to the definition of the *n*-Krylov's subspace

$$\underline{KS}_n = \underline{\underline{C}}^n\,\underline{R} \qquad [54]$$

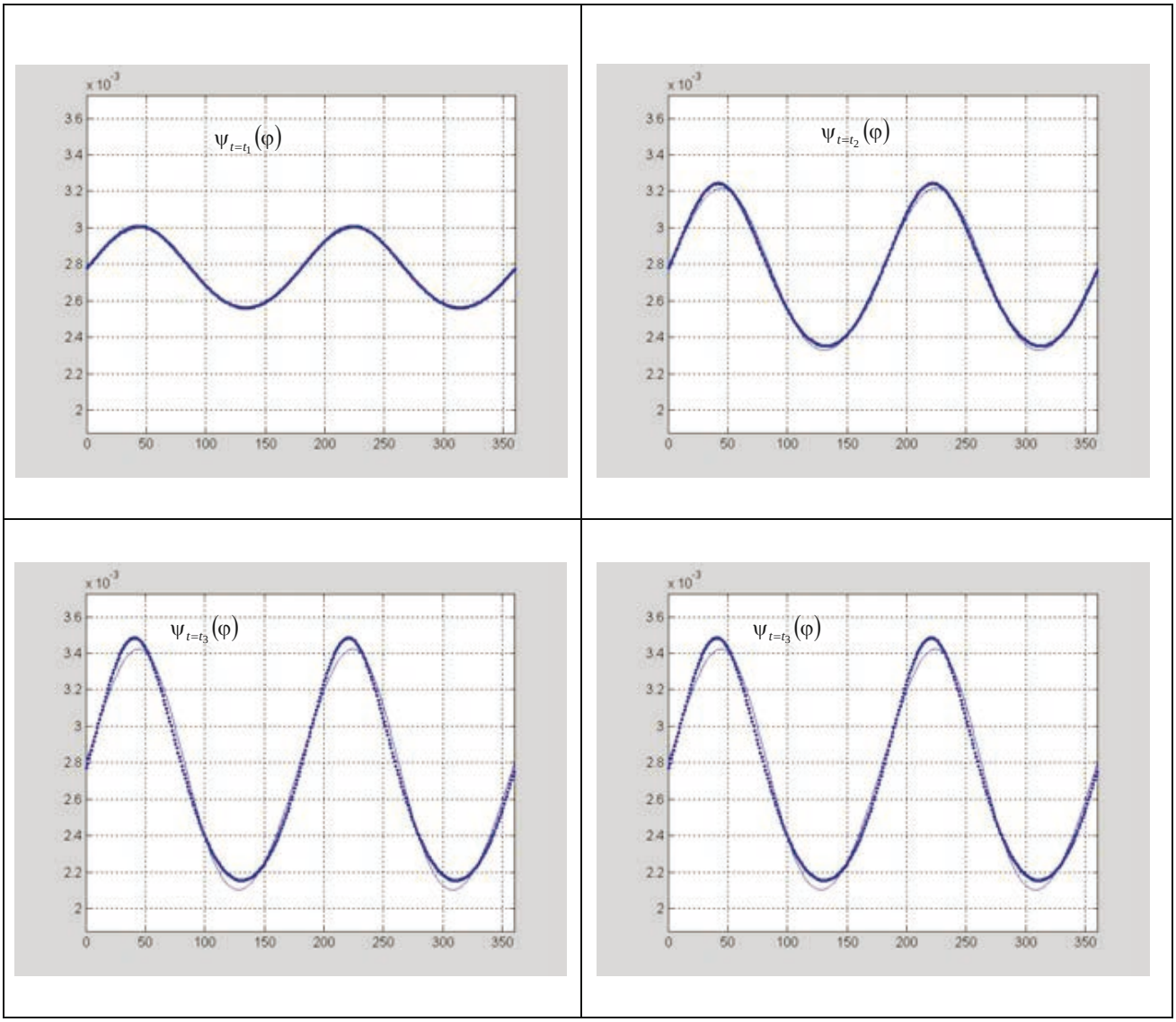

Figure 6. Fiber orientation distribution for a suspension of fibers with *k=0.8*: reduced order solutions versus the reference ones.

Now, we consider the approximation basis enrichment using the first three Krylov's subspaces shown in figure 7, that have been computed at the time related to the solution depicted in figure 6 (subfigure right-down).

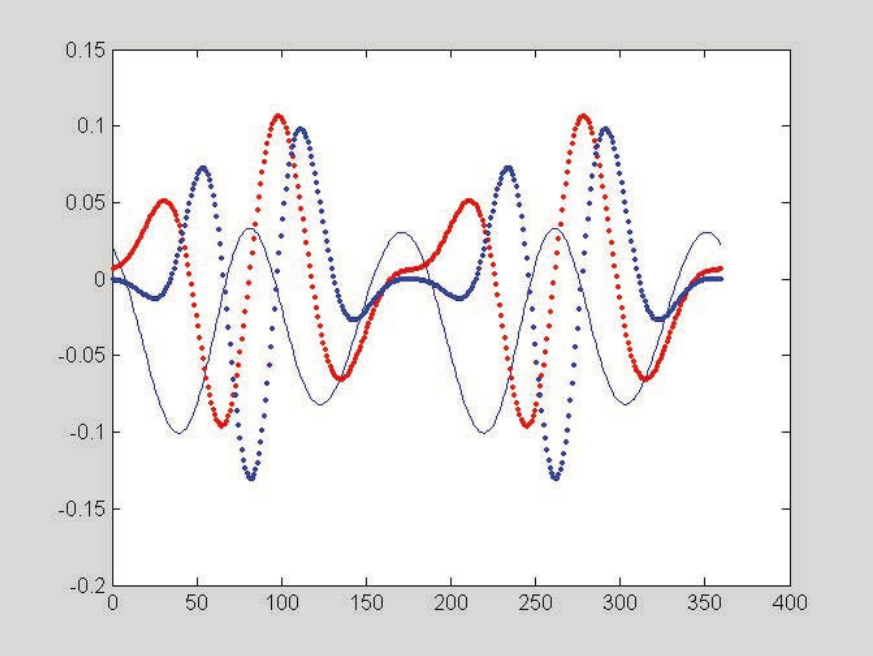

Figure 7. Three first Krylov's subspaces related to the low order solution at time t_4.

When the evolution of the fiber orientation distribution is computed again using the basis obtained by adding to the previous one the three Krylov's subspaces shown in figure 7, we obtain at the last time step (t_4) the solution shown in figure 8. In this case the enriched low-order solution (curve in red) fits much more better the reference solution than the one obtained by using the low-order basis before the enrichment (doted blue curve).

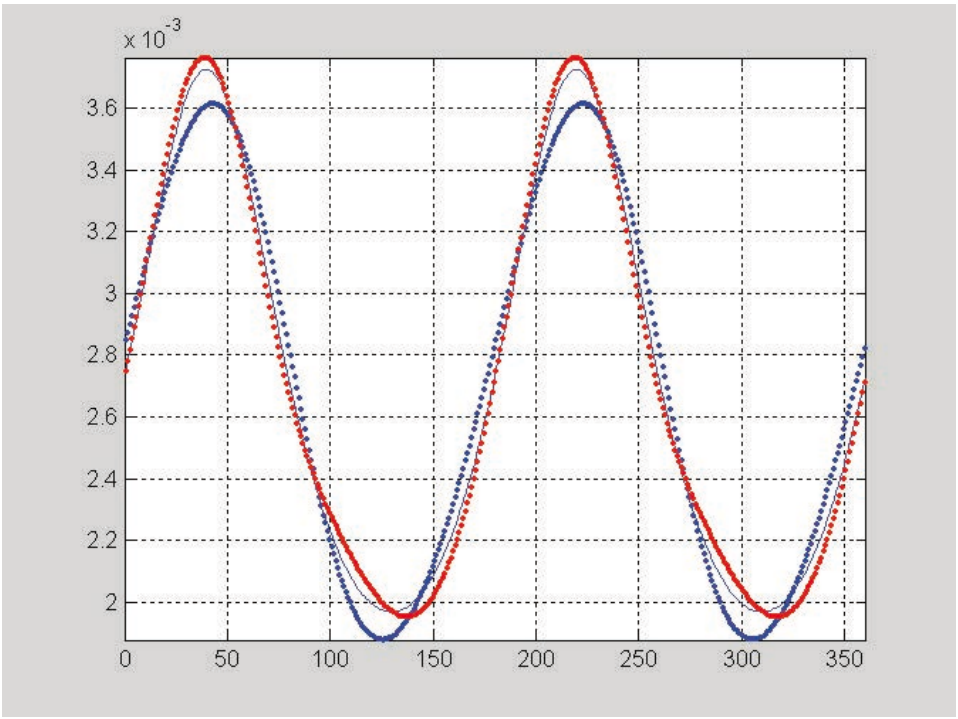

Figure 8. Low-order solution (with –red curve- and without –blue curve- basis enrichment) versus the reference solution (continuous blue curve) at time t_4.

6. Conclusions

The use in tandem of a NEM for solving the macroscopic flow kinematics and a more specific technique for solving the kinetic theory problem related to the microstructure evolution seems to be a powerful tool for simulating complex flows.

REFERENCES

S.G. Advani, Ch.L. Tucker III. Closure Approximations for Three-dimensional Structure Tensors, J. Rheol., 34, 367-386, (1990).

A . Ammar, F. chinesta. A Particle Strategy for Solving the Fokker-Planck Equation Governing the Fiber Orientation Distribution in Steady Recirculating Flows Involving Short Fiber Suspensions. Lectures Notes on Computational Science and Engineering, Springer, In press.

J. Azaiez, K. Chiba, F. Chinesta, A. Poitou. State-of-the-Art on Numerical Simulation of Fiber-Reinforced Thermoplastic Forming Processes. Archives of Computational Methods in Engineering, 9/2, 141-198, (2002).

G.K Batchelor. Slender-body Theory for Particles of Arbitrary Cross-section in Stokes Flow, J. Fluid Mech., 44, 419-440, (1970).

G.K. Batchelor. The Stress Generated in Non-Dilute Suspensions in Elongated Particles by Pure Straining Motion, J. Fluid Mech., 46, 813-829, (1971).

C.V. Chaubal, A. Srinivasan, O. Egecioglu, L.G. Leal. Smoothed Particle Hydrodynamics Techniques for the Solution of Kinetic Theory Problems. Part 1: Method. Journal of Non-Newtonian Fluid Mechanics, \70, 125-154, (1997).

K. Chiba, K. Nakamura. Numerical Solution of Fiber Suspension Flow Through a Complex Channel, J. Non-Newtonian Fluid Mech., 78, 167-185, (1998).

K. Chiba, A. Ammar, F. Chinesta. On the Fiber Orientation in Steady Recirculating Flows Involving Short Fibers Suspensions. Submitted to Rheologica Acta, (2004).

F. Chinesta, G. Chaidron, A. Poitou. On the Solution of the Fokker-Planck Equations in Steady Recirculating Flows Involving Short Fiber Suspensions. Journal of Non-Newtonian Fluid Mechanics, 113/2-3, 97-125, (2003).

E. Cueto, N. Sukumar, B. Calvo, J. Cegoñino, M. Doblaré, Overview and Recent Developments in Natural Neighbour Galerkin Methods, Archives of Computational Methods in Engineering, 10/4, 307-384, (2003).

F. Dupret, V. Verleye, B. Languillier. Numerical Prediction of the Moulding of Short Fiber Composite Parts, First ESAFORM Conference on Material Forming, Sophia-Antipolis, France (1998).

F. Folgar, Ch.L. Tucker III. Orientation Behaviour of Fibers in Concentrated Suspensions, J. Reinf. Plast. Composites, 3, 98-119 (1984).

D. Gonzalez, E. Cueto , M. Doblare. Volumetric Locking in Natural Neighbour Galerkin Methods. International Journal for Numerical Methods in Engineering, In press, (2004).

E.J. Hinch, L.G. Leal. Constitutive Equations in Suspension Mechanics. Part I, J. Fluid Mech., 71, 481-495, (1975).

E.J. Hinch, L.G. Leal. Constitutive Equations in Suspension Mechanics. Part II, J. Fluid Mech., 76, 187-208, (1976).

G.B. Jeffery. The Motion of Ellipsoidal Particles Immersed in Viscous Fluid, Proc. Royal Soc., A 102, p. 161 (1922).

M.A. Martinez, E. Cueto, M. Doblaré, F. Chinesta. Natural Element Meshless Simulation of Injection Processes Involving Short Fiber Suspensions. Journal of Non-Newtonian Fluid Mechanics, 115, 51-78, (2003).

M.A. Martinez, E. Cueto, I. Alfaro, M. Doblaré, F. Chinesta. Updated Lagrangian Free Surface Flow Simulations with the Natural Neighbour Galerkin Methods. International Journal for Numerical Methods in Engineering, In press, (2004).

F. Meslin, A. Poitou. Viscosité en Cisaillement d'un Composites Fibres Courtes à l'Etat Fondu, C.R. Acad. Sci. Paris, 327, 559-565, (1999).

H.M. Park, D.H. Cho. The Use of the Karhunen-Loève Decomposition for the Modelling of Distributed Parameter Systems, Chem. Engineer. Science, 51, 81-98, (1996).

O. Pironneau. Finite Elements Methods for Fluids, Wiley (1989).

D. Ryckelynck.A Priori Model Reduction Method for the Optimization of Complex Problems, Workshop on Optimal Design of Materials and Structures, Ecole Polytechnique, Palaiseau, Paris (France), November (2003).

D. Ryckelynck. A Priori Hyperreduction Method: an Adaptive Approach, Submitted to the Journal of Computational Physics, (2004).

N. Sukumar, B. Moran and T. Belytschko. The Natural Element Method in Solid Mechanics, International Journal for Numerical Methods in Engineering, 43/5, 839-887, (1998).

M. Sussman, P. Smereka, S. Osher. A Level Set Approach to Computing Solutions to Incompressible Two-Phase Flows, J. Comput. Phys., 114 (1994).

Ch.L. Tucker III. Flow Regimes for Fiber Suspensions in Narrow Gap, J. Non-Newtonian Fluid Mech., 39, 239-268, (1991).